



OPEN Dual-directional epi-genotoxicity assay for assessing chemically induced epigenetic effects utilizing the housekeeping *TK* gene

Haruto Yamada¹, Mizuki Odagiri¹, Keigo Yamakita¹, Aoi Chiba¹, Akiko Ukai², Manabu Yasui²✉, Masamitsu Honma², Kei-ichi Sugiyama², Kiyoe Ura¹ & Akira Sassa¹✉

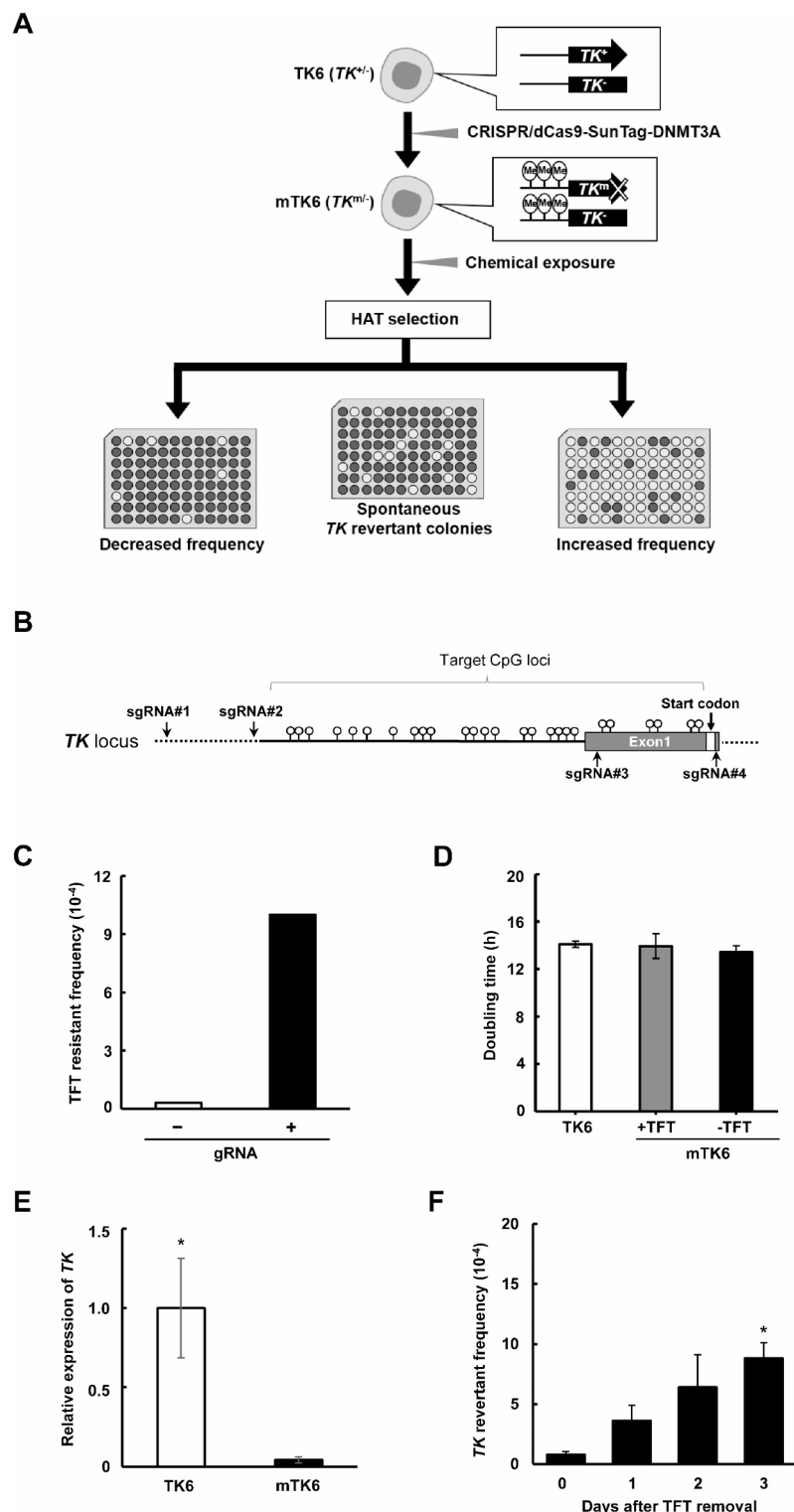
Numerous chemicals are associated with carcinogenesis through epigenetic alterations in cells. To detect global epigenetic changes induced by carcinogens, the housekeeping gene can serve as a reporter locus, offering a baseline for identifying shifts in epigenetic marks. To investigate this potential, we developed a simple, cost-effective, and quantitative reporter system to assess chemically induced epigenetic effects, utilizing the thymidine kinase (*TK*) gene mutation assay as a foundation. Using a standard genotoxicity test cell line, human lymphoblast TK6, we edited the CpG promoter loci of the endogenous *TK* gene using the CRISPR/dCas9-SunTag-DNMT3A system. This epi-genotoxicity assay, employing modified mTK6 cells, provides a simple method for quantifying chemically induced epigenetic effects. The assay successfully detects both increased TK reversion rates induced by DNMT inhibitors, such as 5-Aza-2'-deoxycytidine and GSK-3484862, and, for the first time, a significant reduction in TK revertant frequency caused by the non-genotoxic carcinogen 12-O-tetradecanoylphorbol-13-acetate (TPA). Chromatin immunoprecipitation and western blotting analyses revealed that TPA treatment led to a global decrease in H3K27Ac levels, likely driven by TPA-mediated inflammation. These results demonstrate the utility of the epi-genotoxicity assay as a valuable tool for evaluating dual-directional epigenetic changes triggered by chemical exposure.

Keywords Toxicology, Epi-genotoxicity, Reporter assay, 12-O-tetradecanoylphorbol-13-acetate, DNMT inhibitor, *TK* gene

Numerous chemical agents have been implicated in carcinogenesis through diverse mechanisms, including genetic, epigenetic, and metabolic alterations. Among these processes, the ability of chemicals to induce genetic changes is defined as genotoxicity. Genotoxic agents can bind directly to DNA and act indirectly by interfering with enzymatic pathways such as DNA replication, DNA repair, and DNA damage signaling, ultimately leading to gene mutations and chromosomal aberrations. The potential risk of chemicals interacting with DNA is evaluated through genotoxicity testing. The Organization for Economic Co-operation and Development (OECD) has established guidelines for assessing chemicals using *in vitro* genotoxicity tests, including the bacterial Ames test, the mammalian cell chromosomal aberration test, and the mammalian cell gene mutation test¹.

In addition to genotoxic potential, epigenetic alterations are believed to contribute to chemically induced carcinogenesis². Among these, cytosine C5 methylation in CpG dinucleotides represents a key epigenetic modification, playing crucial roles in processes such as X chromosome inactivation, genomic imprinting, and repression of retrotransposons through gene silencing. In mammals, DNA methylation is catalyzed by DNA methyltransferases (DNMTs). Of the active DNMTs, DNMT1 is responsible for maintaining DNA methylation during replication, while DNMT3A/3B are involved in *de novo* DNA methylation under specific cellular conditions. Beyond DNA methylation, gene expression is further regulated by post-translational histone modifications, which serve as structural elements for packaging genomic DNA within the nucleus. Histone H3K4 trimethylation (H3K4me3) and H3K27 acetylation (H3K27Ac) are transcriptionally active marks that exhibit an inverse correlation with DNA methylation at gene promoter regions. These cellular epigenetic patterns

¹Department of Biology, Graduate School of Science, Chiba University, Chiba 263-8522, Japan. ²Division of Genome Safety Science, National Institute of Health Sciences, 3-25-26 Tonomachi, Kawasaki-ku, Kawasaki-shi 210-9501, Kanagawa, Japan. ✉email: m-yasui@nihs.go.jp; a-sassa@chiba-u.jp



can be influenced by exposure to certain chemical reagents that directly or indirectly modify DNA methylation and/or histone modifications³.

Several therapeutic drugs have been developed as epigenetic modifiers with anticancer potential. Aberrant DNA methylation and the hyperactivation of histone deacetylases (HDACs) are closely linked to cell proliferation and metastasis in various cancers, making DNMTs and HDACs promising therapeutic targets⁴. 5-Aza-2'-deoxycytidine (5-azadC) is a widely used demethylating agent that inhibits DNMTs through its incorporation into genomic DNA⁵. Similarly, HDAC inhibitors promote hyperacetylation of core histones, thereby modulating chromatin structure and altering gene expression patterns⁶. Beyond these designed therapeutic agents, environmental chemicals such as bisphenol A, arsenic, cadmium, benzene, and pesticides have been reported to induce aberrant epigenetic changes, contributing to the onset of various diseases⁷. Notably, many carcinogens are believed to exert their effects through non-genotoxic mechanisms⁸. Therefore, evaluating the potential

Fig. 1. Establishment of the epi-TK assay using epigenome-edited human lymphoblast TK6 cells. **(A)** Overview of the epi-TK assay. Based on human TK6 cells, site-specific methylation of CpG sites in the promoter region of the *TK* gene achieved via the CRISPR/dCas9-SunTag-DNMT3A system. The resulting mTK6 cell line was cultured in medium containing TFT. After exposure to test compound, the cells were seeded into 96-microwell plates with HAT to assess TK revertant frequency. The cells were plated into 96-microwell plates without HAT to determine CE. Colony numbers from CE and HAT plates were recorded, and the TK revertant frequency was calculated as described in the Methods section. **(B)** Target CpG loci within the promoter region of the *TK* gene, with the positions of gsRNAs indicated by arrowheads. The sequences of gsRNAs are listed in Supplementary Table S1. **(C)** Representative data showing the TFT resistant frequency after transfection with plasmids encoding CRISPR/dCas9-SunTag-DNMT3A and sgRNAs. The frequency of TFT-resistant colonies was assessed following transient expression of CRISPR/dCas9-SunTag-DNMT3A and sgRNAs targeting the *TK* gene (+). Transfection with the CRISPR/dCas9-SunTag-DNMT3A plasmid and an empty sgRNA vector served as negative control (-). **(D)** Population doubling time of TK6 and mTK6 cells. Doubling time were measured in both the absence or presence of TFT. **(E)** Expression levels of the *TK* gene in TK6 and mTK6 cells. Relative mRNA abundance was normalized to *GAPDH* expression. **(F)** Spontaneous TK revertant frequency of mTK6 cells. Cells were seeded at a concentration of 2,000 cells/mL in the presence of HAT into 96-microwell plates. Cells were also plated in 96-microwell plates at a density of 8 cells/ml without HAT selection to assess the cloning efficiency (CE). After 21 days of incubation, the number of colonies in both the CE and HAT plates was recorded. TK revertant frequencies were determined as described in the Methods section. Data are presented as the mean \pm S.E. of three independent experiments. * A Significant difference between the assessed cells; $P < 0.05$ (Dunnett's Multiple Comparison Test).

epigenetic effects and underlying mechanisms of action is a critical component in the safety assessment of environmental chemical compounds.

To evaluate epigenetic alterations induced by chemical reagents, researchers have developed various cell-based reporter assays. Johnson et al. introduced a system using an epigenetically silenced green fluorescent protein (*GFP*) reporter gene controlled by an exogenous cytomegalovirus promoter⁹. More recently, endogenous tumor suppressor genes such as *SFRP1* and *BRCA1* have been employed as *GFP*-based reporters to study epigenetic changes^{10,11}. Similarly, Okochi-Takada et al. developed a high-throughput screening platform using luciferase and *GFP* reporter genes driven by the inactivated *UCHL1* locus in HCT116 cells¹². These systems generally detect epigenetic modifications in unidirectional manner, either inactivation or reactivation of gene expression, based on the initial epigenetic state of the reporter gene locus. A notable approach is an *in vitro* reporter system utilizing DNMT-transformed yeast cells, enabling rapid and efficient bidirectional detection of epigenetic silencing and activation caused by chemical reagents^{13–15}. However, to ensure the extrapolation of experimental results to humans, a flexible bidirectional reporter assay needs to be designed in mammalian cells to effectively detect diverse modifications resulting from chemical exposure. Currently, the epigenetic impacts of chemicals on housekeeping genes remain poorly understood, emphasizing the need to evaluate these genes as potential reporter loci to broaden the scope and utility of such assays.

In this study, we aimed to develop an epi-genotoxicity assay to evaluate epigenetic modifications induced by carcinogens, based on the thymidine kinase (*TK*) gene mutation assay (TK assay) technique. The TK assay is a conventional mammalian *in vitro* genotoxicity test that detects various mutations at the housekeeping *TK* gene locus, utilizing the human lymphoblastoid TK6 cell line¹⁶. The OECD Test Guideline (TG490) adopted the conventional TK assay for the safety assessment of pharmaceutical, industrial, agricultural, and environmental chemicals¹⁷. We recently enhanced the TK assay by developing genome-edited TK6 cell lines, improving its sensitivity for detecting genotoxic and cytotoxic effects of chemicals^{18–20}. In the current study, we further advanced this approach by establishing epigenetically modified TK6 derivative (mTK6) cells as the epi-genotoxicity test system. Using the CRISPR/dCas9-SunTag-DNMT3A system, CpG sites within the endogenous *TK* promoter region were selectively methylated²¹, resulting in mTK6 cells with a stably methylated *TK* gene. These cells can be propagated in the presence of trifluorothymidine (TFT), which selectively exerts cytotoxicity against *TK*-proficient cells. The developed method, termed the “epi-TK assay,” enables accurate quantification of epigenetic changes induced by chemical exposure. This is achieved by measuring the frequency of TK revertant colonies in hypoxanthine, aminopterin, and thymidine (HAT) selection medium (Fig. 1A).

To assess the ability of the epi-TK assay to quantify global epigenetic effects, we tested DNMT inhibitors (5-azadC and GSK-3484865) and HDAC inhibitors (vorinostat and trichostatin A) as model substances with well-characterized mechanisms of action (Fig. S1). Additionally, we examined the epigenetic effects of 12-O-tetradecanoylphorbol-13-acetate (TPA), a widely studied non-genotoxic tumor promoter/inflammation inducer derived from the seed oil of *Jatropha curcas* L. Using the established epi-TK assay, we observed not only an increase in TK reversion frequency induced by 5-azadC and GSK-3484865 but also a significant decrease in TK revertant frequency following TPA exposure. Chromatin immunoprecipitation and western blotting analyses revealed that TPA treatment caused a global reduction in H3K27Ac levels, likely linked to TPA-mediated chronic inflammation. These findings highlight the utility of the epi-genotoxicity assay as a tool for evaluating epigenetic alterations induced by chemical exposure in both directions.

Results

Establishment of human TK6 derivative cells assessing chemical-induced epigenetic alterations

We developed a reporter system to assess chemical-induced epigenetic alterations using the mammalian *TK* gene mutation assay as a platform. To create a cell line capable of quantifying epigenetic effects, we employed CRISPR/dCas9-SunTag-DNMT3A along with sgRNA expression plasmids specifically designed to methylate CpG loci within the promoter region of the endogenous *TK* gene (Fig. 1B). As illustrated in Fig. 1C, transient expression of the sgRNAs resulted in a significant increase in TFT-resistant colonies (1.0×10^{-3}) compared to cells transfected with empty sgRNA vectors (3.2×10^{-5}). Among 12 clones isolated, we selected a representative clone that exhibited stable proliferation in TFT-containing medium. This isolated clone, designated as the “mTK6” cell line, had a population doubling time of 14 ± 1.0 h in the absence of TFT and 13 ± 0.52 h in its presence, similar to the original TK6 cell line's doubling time of 14 ± 0.26 h (Fig. 1D). RT-qPCR analysis revealed abolished *TK* gene expression in mTK6 cells compared to TK6 cells (Fig. 1E), indicating that *TK* gene expression was repressed due to DNA methylation in its promoter region. We also evaluated the TK revertant frequency during cell proliferation up to 3 days following TFT removal from the medium (Fig. 1F). The TK revertant frequency was determined by counting HAT-resistant colonies seeded in 96-microwell plates. Spontaneous TK reversion was observed in a time-dependent manner: 0 day ($0.77 \pm 0.27 \times 10^{-4}$), 1 day ($3.6 \pm 1.3 \times 10^{-4}$), 2 days ($6.4 \pm 2.7 \times 10^{-4}$), and 3 days ($8.8 \pm 1.3 \times 10^{-4}$). Based on this background TK revertant frequency, we hypothesize that epigenetic alterations induced by chemical exposure can be quantified by measuring changes in the number of TK revertant colonies. It should be noted that the CRISPR/dCas9-SunTag-DNMT3A system has been reported to exhibit minimal off-target effects²¹. Additionally, the major potential off-target sites for *TK* gRNA #1–4 are located within intergenic and intronic regions in the human genome, where off-target DNA methylation is unlikely to affect the quality of the TK reporter assay.

Quantification of epigenetic effects of covalent and non-covalent DNA methyltransferase inhibitors.

We first evaluated the capability of the epi-TK assay to quantify the effects of typical DNA demethylating agents. 5-AzadC, a widely used potent DNMT inhibitor, was tested on mTK6 cells across a range of concentrations (0.02 – 0.1 μ M), determined based on cytotoxicity assays (Fig. 2A). Since many epigenetic modifications are coupled with DNA replication²², extreme cytotoxicity that impairs cell proliferation may hinder the accurate measurement of epigenetic effects. Thus, the cytotoxicity of test substances was assessed based on relative survival (%), defined as the colony formation efficiency of cells plated immediately after chemical treatment. The relative survival of mTK6 cells was approximately 80–60% and 90–30% after exposure to increasing concentrations of 5-azadC and GSK-3484862, respectively (Fig. 2A,C), indicating moderate cytotoxicity at higher concentrations. As shown in Fig. 2B, treatment with 5-azadC led to a 230-fold increase in TK revertant frequency ($7.7 \pm 1.0 \times 10^{-2}$) at the highest concentration (0.1 μ M) compared to the solvent control ($3.3 \pm 0.67 \times 10^{-4}$), corresponding to 0 μ M 5-azadC in Fig. 2B. Notably, 5-azadC is known for its high cytotoxicity and genotoxicity due to the formation of covalent DNA-DNMT adducts. To evaluate the assay's versatility, we tested the epigenetic effects of non-covalent DNMT inhibitor GSK-3484862. As shown in Fig. 2D, GSK-3484862 treatment significantly increased TK revertant frequency in a dose-dependent manner (0.12 ± 0.033 at 0.5 μ M, 0.19 ± 0.052 at 2.0 μ M, and 0.29 ± 0.044 at 5.0 μ M) compared to the DMSO control ($1.6 \pm 0.46 \times 10^{-4}$), corresponding to 0 μ M GSK-3484862 in Fig. 2D.

We next investigated the DNA methylation pattern of the *TK* gene promoter region in mTK6 cells. Bisulfite sequencing revealed methylation of cytosine at 26 CpG dinucleotides within a 230 bp region upstream of the start codon in both *TK* alleles (Fig. 2E). To further examine the methylation status of the *TK* promoter after exposure to DNMT inhibitors, we analyzed TK revertant colonies. Notably, all CpG sites within the *TK* promoter were unmethylated in both spontaneous and DNMT inhibitor-mediated (5-azadC and GSK-3484862) TK revertant colonies. These findings suggest that the DNA methylation pattern of the *TK* promoter is closely associated with its gene expression status.

Determination of histone modification status in the methylated *TK* gene promoter

Transcriptionally active chromatin is characterized by the presence of H3K27ac and H3K4me3 near the transcription start site of the target gene. Thus, we investigated whether the status of H3K27ac and H3K4me3 was altered following DNA methylation in the *TK* promoter region. Interestingly, ChIP-qPCR analyses revealed that enrichment levels of H3K27ac and H3K4me3 were comparable to those observed in TK6 cells (Fig. 3A and B). Consistent with these findings, exposure to HDAC inhibitors vorinostat (0.2 μ M) and trichostatin A (0.01 μ M) for 24 and 48 h did not affect the frequency of TK revertants (Fig. 3C). This lack of effect may be due to the sustained levels of H3K27ac and H3K4me3 in the presence of repressive DNA methylation at the *TK* promoter region in mTK6 cells.

Detection of the epigenetic consequence of a non-genotoxic carcinogen/inflammation inducer 12-O-tetradecanoylphorbol-13-acetate

Based on the unique epigenetic pattern of the *TK* gene in mTK6 cells described above, we hypothesized that chemically induced global histone modifications could be detected through changes in the frequency of TK reversion. To test this hypothesis, we selected TPA, a potent non-genotoxic carcinogen with potential effects on histone modifications, though the persistent epigenetic consequences remain poorly understood. As shown in Fig. 4A, treatment with TPA at concentrations ranging from 0.02 to 1.0 μ g/ml resulting in approximately 40–50% cell survival. Under these conditions, the frequency of TK revertants decreased significantly, with a maximum of 28-fold reduction ($0.090 \pm 0.0058 \times 10^{-4}$) compared to the solvent control ($2.5 \pm 0.42 \times 10^{-4}$) (Fig. 4B). To further investigate histone modification status following TPA treatment, cells were harvested three days of cultivation

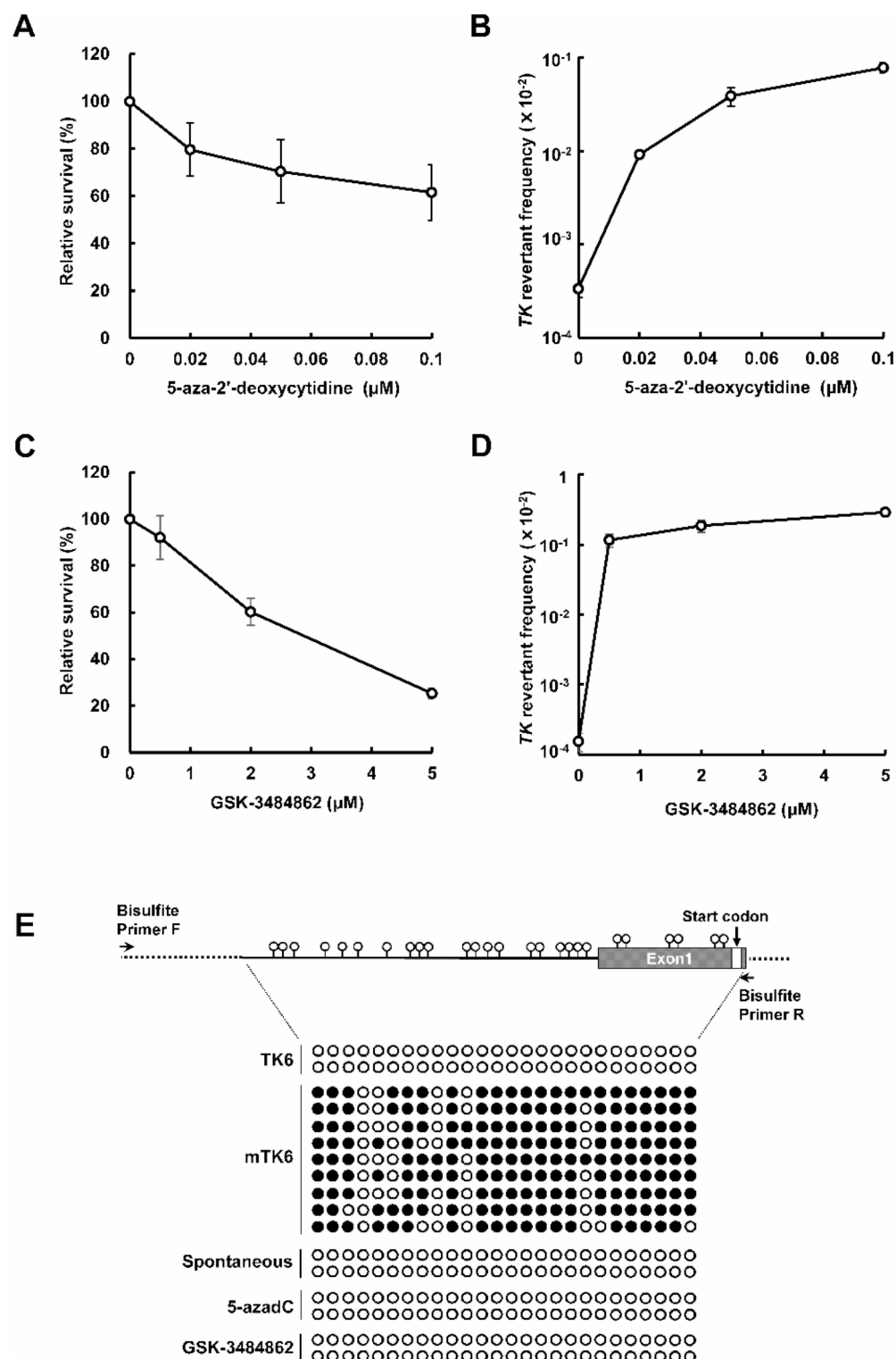


Fig. 2. Relative survival and TK revertant frequency in the epi-TK assay for 5-aza-2'-deoxycytidine and GSK-3484862. Cytotoxic and epigenetic effects were measured as relative survival (%) and TK revertant frequency ($\times 10^{-2}$), respectively, following treatment with 5-azadG (A, B) and GSK-3484862 (C, D). The data on TK revertant frequencies were statistically analyzed using Dunnett's test and compared to the solvent control. Results from three independent experiments are presented. (E) Bisulfite sequencing analysis of the *TK* gene in mTK6 cells. Each circle represents a CpG site located within or near the promoter region of the *TK* gene. Black circles indicate methylated CpG site, while white circles represent unmethylated CpG site. Each row corresponds to the CpG sites of a single clone. Arrows indicate primers for bisulfite sequencing.

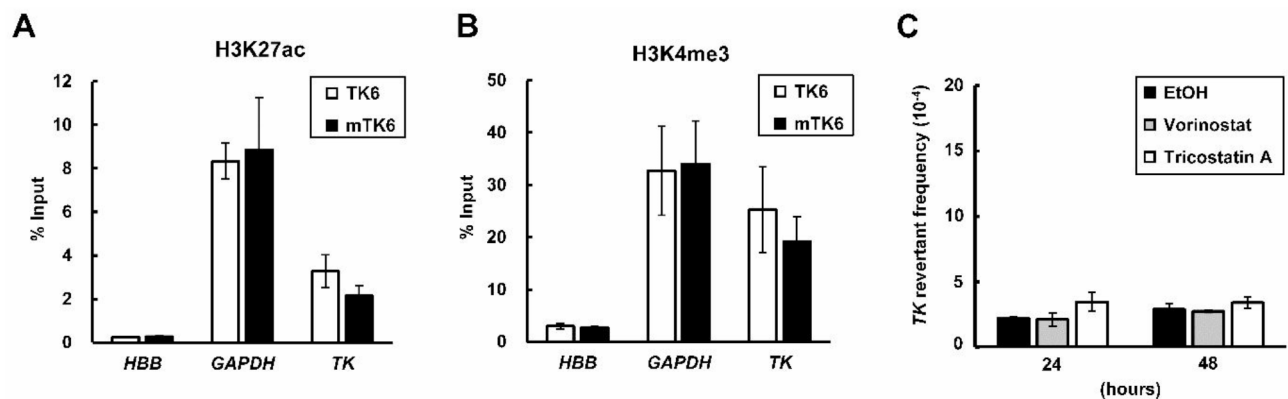


Fig. 3. Histone modification status of the *TK* gene. Active histone marks H3K27Ac (A) and H3K4me3 (B) at the transcription start site of the *TK* gene were analyzed by chromatin immunoprecipitation and qPCR analysis. The *HBB* and *GAPDH* genes were analyzed for comparison. (C) TK revertant frequencies following treatment with HDAC inhibitors vorinostat and trichostatin A. Ethanol (EtOH) served as a negative control. Data are presented as the mean \pm S.E. of three independent experiments.

following the exposure to TPA and subjected to ChIP-qPCR and western blotting analysis. ChIP-qPCR analysis revealed a significant reduction in H3K27Ac levels at the *GAPDH* and *TK* loci after TPA exposure (Fig. 4C). In contrast, the enrichment of H3K4me3 did not significantly change between ethanol- and TPA-treated cells (Fig. 4D). Consistently, western blotting analysis confirmed a significant reduction in H3K27Ac levels following TPA treatment (Fig. 4E,F).

According to a recent study, differential gene expression patterns of epigenetic regulators, including DNMTs and chromatin remodelers, were observed depending on the duration of TPA exposure²³. To investigate whether the reduction in H3K27Ac levels observed in our results is due to altered expression of epigenetic modulators, we performed RNA-seq analysis to identify DEGs resulting from TPA treatment. A 24-h treatment with TPA led to the upregulation of genes associated with the “ERK1 and ERK2 cascade” and “MAPK cascade,” followed by the “inflammatory response” (Fig. S2A–E). After washing out TPA and culturing the cells for 3 days, Gene Ontology analysis revealed that the biological pathways of upregulated genes were enriched in “leukocyte activation,” “innate immune response,” and “lymphocyte activation.” For the downregulated genes associated with TPA treatment, fewer pathways were enriched: “leukocyte tethering or rolling” for the 24-h TPA treatment, and “regulation of cell migration,” “cellular response to chemokine,” and “leukocyte activation” for the 3-day culture following TPA treatment. No significant differential expression of genes involved in epigenetic regulation, such as DNMT1, DNMT3A/B, histone acetyltransferases, and HDACs, was observed.

Discussion

Over the past two decades, next-generation sequencing-based technologies have been developed to explore the epigenetic regulatory landscape of cells and tissues. Pioneered by Bisulfite-seq and ChIP-seq detecting DNA methylation and histone modifications, a wide range of epigenome profiling techniques has developed. These include Micrococcal Nuclease sequencing (MNase-seq), DNase I hypersensitive site sequencing (DNase-seq), Formaldehyde-assisted isolation of regulatory elements sequencing (FAIRE-Seq), and Assay for Transposase-Accessible Chromatin sequencing (ATAC-seq), all of which are commonly used to assess chromatin accessibility^{24–27}. An emerging technology, Hi-C (high-resolution chromosome conformation capture), provides a high-throughput method for mapping the 3D structure of chromosomes within the nucleus²⁸. While these techniques have advanced epigenetic research, their implementation requires considerable experimental and analytical expertise, as well as expensive instruments and reagents. In this context, the development of reporter assays to detect specific patterns of epigenetic alteration offers a simpler, more cost-effective, and quantitative approach for evaluating chemical toxicity, providing framework for such assays. Thus, the experimental procedure of the epi-TK assay (Fig. 1A), based on the standard genotoxicity testing outlined in OECD TG490, meets the criteria for an effective reporter system, contributing to safety assessment. Currently, no standardized methods for evaluating epigenetic effects are included in the OECD guidelines. The epi-TK assay holds potential as a valuable approach for toxicity assessment.

For the development of the epi-TK assay, CRISPR/dCas9-SunTag-DNMT3A was transiently expressed in TK6 cells, leading to increased DNA methylation at CpG dinucleotides within the *TK* promoter region (Fig. 2E). Given that the expression of the *TK* gene is regulated by transcription factors such as E2F1 and SP1^{29,30}, it is likely that DNA methylation at these CpG loci inhibits the binding of transcription factors, thereby preventing

the transcription of the *TK* gene. Interestingly, the spontaneous frequency of TK revertant increased with the duration of cell culture after the removal of TFT (Fig. 1F), suggesting that the CpG sites in the promoter region were spontaneously demethylated during cell division. This reversible state of the epigenetically edited *TK* gene may be attributed to the persistent presence of active histone marks, such as H3K27Ac and H3K4me3 (Fig. 3A,B). Moreover, a recent study demonstrated that artificially introduced histone modifications, including H3K4me3, H3K27Ac, H3K27me3, H3K9me2/3, and H2AK119Ub, are progressively diluted after cell division³¹. Although the mechanistic basis of such epigenetic restoration remains unclear, a potential regulatory mechanism could involve the three-dimensional chromatin architecture within the nucleus³². Nevertheless, the epigenetic state of the *TK* gene is stably maintained when cells are cultured in the presence of TFT (Fig. 1D), ensuring the reproducibility of the assay.

Using the housekeeping *TK* gene as a reporter locus, the effects of DNMT inhibitors were quantified (Fig. 2). GSK-3484862 exhibited a stronger inhibitory effect on DNA methylation compared to 5-azadC at the maximum concentration. Notably, GSK-3484862 can be used at higher concentrations due to its lower cytotoxicity, further enhancing its effectiveness in reducing DNA methylation levels. These results align with the observation that GSK-3484862 induces demethylation more efficiently than 5-azadC in murine cells³³. This difference in demethylating efficacy is attributed to the cytotoxicity of 5-azadC, which forms covalent protein-DNA adducts³⁴, whereas GSK-3484862 inhibits DNMT1 in a non-covalent manner. Regarding HDAC inhibitors, treatment of mTK6 cells with trichostatin A and vorinostat did not significantly increase the TK revertant frequency (Fig. 3C), likely due to the persistent levels of H3K27Ac and H3K4me3 at the *TK* gene locus.

TPA stimulates cellular responses, including cell proliferation, migration, and differentiation through the activation of specific types of protein kinase C (PKC)^{35–37}. Previous reports have shown that TPA treatment rapidly increases H3S10/H3S28 phosphorylation and H3 acetylation levels via mitogen- and stress-activated protein kinases^{38–40}. These responses are associated with the transcriptional activation of immediate early response genes, with phosphorylation of both serine residues peaking around 1 h following TPA treatment and then declining^{38,39}. Interestingly, in our study, treatment of cells with TPA resulted in a significant decrease in TK reversion frequency (Fig. 4B), accompanied by a global reduction in H3K27Ac levels (Fig. 4C–F). The differences observed in our study may be due to the varying time scales used to assess histone modifications following TPA exposure. Specifically, H3K27Ac and H3K4me3 levels were measured after a 3-day recovery period following TPA treatment, allowing to distinguish immediate-early responses from persistent epigenetic changes. In agreement with our findings, prolonged TPA exposure leads to a global reduction of H3S10 phosphorylation in HepG2 cells⁴¹. Therefore, the TPA-induced reduction in H3K27Ac may reflect changes distinct from the histone modifications involved in the immediate-early responses to cellular stimuli.

Initially, we hypothesized that TPA exposure might induce changes in the expression of epigenetic regulators as a potential mechanism behind the observed epigenetic alterations. Supporting this idea, a recent study reported that transcriptome analysis of Bhas 42 cells exposed to TPA revealed altered expression patterns of key epigenetic factors, including *DNMT1*, *DNMT3A*, *MBD3*, and *Mi2*²³. However, in our study, TPA treatment did not induce DEGs in epigenetic-related pathways, such as those involving DNMTs, HDACs, and histone acetyltransferases (Fig. S2 D and E). Thus, the decreased levels of H3K27Ac are not due to changes in the expression of epigenetic factors that directly regulate chromatin status. These differing results may reflect the malignant status of the cells, including mutations or inactivation of tumor suppressor genes and proto-oncogenes. While Bhas 42 cells are characterized by *Tp53* deficiency, TK6 cells retain the native *TP53* gene and are capable of undergoing the normal apoptotic process, which could explain the differential expression pattern observed in response to the tumor promoter TPA.

TPA is known to induce inflammation through activation of the NFκ-B signaling pathway^{42,43}. Notably, inflammatory stresses are closely linked to epigenetic modifications, including DNA methylation and histone acetylation^{44,45}. Chronic inflammatory stress was observed in TPA-treated mTK6 cells even after three days of cultivation following TPA treatment (Fig. S2E), suggesting that TPA-mediated inflammation may contribute to global epigenetic modifications, which resulted in decreased TK revertant frequency. A potential relationship between the progression of inflammation and histone deacetylation has been reported in both *in vitro* and *in vivo* studies^{46–48}. To support this idea, a recent study suggests that chronic inflammation promotes epigenetic reprogramming⁴⁹. While the precise mechanism behind TPA-mediated H3K27Ac reduction remains unclear, this epigenetic alteration could serve as a biological marker for specific inflammatory responses. Further research is needed to elucidate the mechanistic basis of the epigenetic toxicity associated with this chemical reagent.

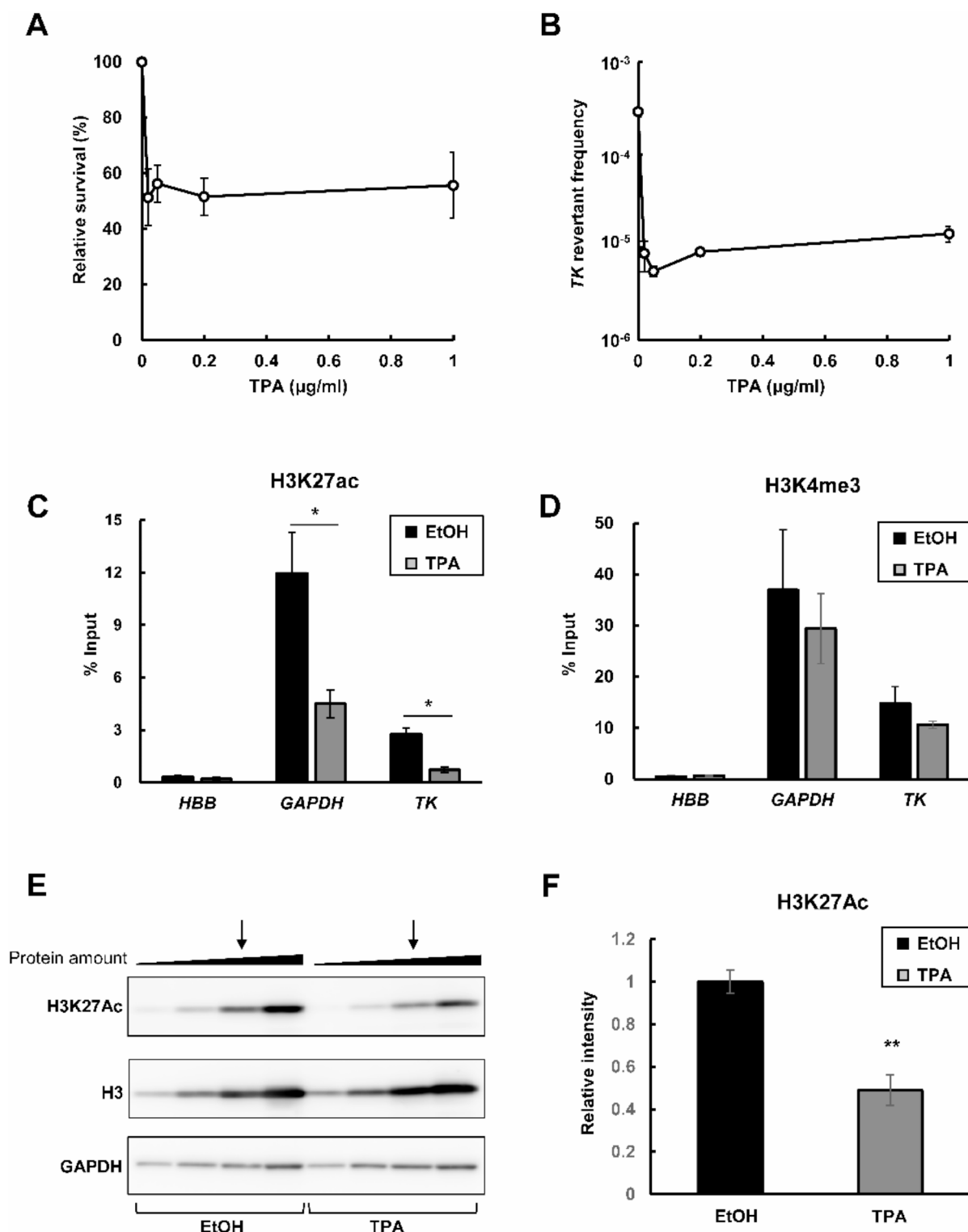
Methods

Cell culture

The human lymphoblastoid TK6 cell line was provided by the Division of Genome Safety Science, National Institute of Health Sciences. The TK6 cell line and its derivative were cultured in RPMI-1640 medium (Nacalai Tesque) supplemented with 200 µg/mL sodium pyruvate, 100 U/mL penicillin, and 100 µg/mL streptomycin, and 10% (v/v) heat-inactivated fetal bovine serum (FBS) (Nichirei Biosciences, Inc.). The cultures were maintained at 37 °C in a 5% CO₂ atmosphere with 100% humidity.

Generation of human mTK6 cell line

To generate TK6 derivative cells with an epigenetically modified *TK* gene, the dCas9-SunTag DNMT3A system was employed to induce DNA methylation at the CpG loci of the *TK* gene promoter. The gRNA cloning vector was generously provided by Dr. George Church (Addgene plasmid #41824; <http://n2t.net/addgene:41824>; RRID: Addgene_41824)⁵⁰ and LLP252 pEF1a-NLS-scFvGCM4-DNMT3a (Addgene plasmid #100941; <http://n2t.net/addgene:100941>; RRID: Addgene_100941) and LLP457 pGK-dCas9-SunTag-BFP (Addgene plasmid# 100957; <http://n2t.net/addgene:100957>; RRID: Addgene_100957) were gift from Dr. Ryan Lister²¹. Four different singl



e-guide RNA (sgRNA) targets were designed for the *TK* promoter region, as detailed in Supplementary Table S1. A plasmid pool consisting of an equimolar mixture of all four sgRNA expression plasmids (21 μg total: 5.25 μg of each plasmid), pGK-dCas9-Suntag-BFP (21 μg), and pEF1a-NLS-scFvGCM4-DNMT3a (8 μg) was transfected into TK6 cells (5×10^6) using 0.1 ml Nucleofector solution V (Lonza) and a Nucleofector 2b device, following the manufacturer's instructions. After 48 h of incubation, the cells were seeded in 200 μl per well into 96-microwell flat bottom plates at concentrations of either 20,000 or 200,000 cells/mL in the presence of 3.0 $\mu\text{g/ml}$ trifluorothymidine (TFT). To determine the plating efficiency, cells were also seeded at a concentration of 8 cells/mL in the absence of TFT. After 10 days of incubation, TFT-resistant clones were isolated and maintained in RPMI-1640 medium containing 3.0 $\mu\text{g/ml}$ TFT for at least 10 passages before preparing frozen stocks. The integrity of the *TK* promoter region sequences in the clones was validated using PCR primers listed in Supplementary Table S2.

◀ **Fig. 4.** Epigenetic effects of 12-O-tetradecanoylphorbol-13-acetate assessed by the epi-TK assay. Cytotoxicity and epigenetic effects were assessed as relative survival (A) and TK revertant frequency (B) after cell treatment with TPA. The data on TK revertant frequencies were statistically analyzed using Dunnett's test and compared to the solvent control. Results from three independent experiments are shown. (C) Enrichment of H3K27Ac in response to TPA treatment. H3K27Ac levels were determined by chromatin immunoprecipitation and qPCR analysis. The *HBB* and *GAPDH* genes were analyzed for comparison. Data are presented as the mean \pm S.E. of three independent experiments. *A significant difference between the assessed samples; $P < 0.05$ (student's t-test). (D) Enrichment of H3K4me3 in response to TPA treatment were determined by chromatin immunoprecipitation and qPCR analysis. Cells were harvested three days of cultivation following the exposure to ethanol or TPA. The *HBB* and *GAPDH* genes were analyzed for comparison. Data are presented as the mean \pm S.E. of three independent experiments. (E) Western blotting analysis for H3K27Ac following TPA treatment. Whole cell extracts were prepared from cells harvested after three days of cultivation following the exposure to ethanol or TPA. Extracted samples were analyzed by immunoblotting and the blots were probed with the indicated antibodies. (F) Quantification of H3K27Ac levels from the western blot shown in (E). The bar graph represents the relative intensity compared to ethanol-treated cells, based on the quantification of the lanes indicated by arrows in (E). Data are expressed as the mean \pm S.E. from three independent biological replicates. **A significant difference between the assessed samples; $P < 0.01$ (student's t-test).

Real-time RT-PCR

Total RNA was extracted from cells using the NucleoSpin RNA Plus kit (Macherey-Nagel). cDNAs were synthesized from the extracted RNA with ReverTra Ace (Toyobo Co., Ltd.). Quantitative PCR was performed using Thunderbird® Next SYBR qPCR Mix (Toyobo Co., Ltd.) and specific primers listed in Supplementary Table S2. The expression levels of the *TK* gene were normalized to the internal *GAPDH* expression levels.

Chemical substances

5-AzadC and vorinostat were obtained from Tokyo Chemical Industry Co., Ltd. (Tokyo, Japan), while trichostatin A was procured from FUJIFILM Wako Pure Chemical Corporation (Osaka, Japan). GSK-3484862 was purchased from ChemieTek (IN, USA), and 12-O-tetradecanoylphorbol-13-acetate (TPA) were sourced from Merck (Darmstadt, Germany). 5-AzadC was dissolved and diluted in H₂O. Trichostatin A, vorinostat, and TPA were dissolved in ethanol, while GSK-3484862 were prepared in dimethyl sulfoxide.

Epi-TK assay

mTK6 cells were cultured to the exponential phase in the presence of 3.0 μ g/ml TFT. Afterward, cells were washed to remove TFT and resuspended in RPMI-1640 medium supplemented with 200 μ g/mL sodium pyruvate and 10% FBS. For chemical exposure, 10 ml aliquots of cell suspension were prepared in 100 mm Petri dishes at a concentration of 250,000 cells/ml. Test chemicals at various concentrations were added to the dishes, which were then incubated at 37°C for 24 h. Following chemical treatment, cells were washed and resuspended in fresh RPMI-1640 medium. To measure the TK revertant frequency, cells were seeded in 200 μ l per well into 96-microwell flat bottom plates containing 200 μ M hypoxanthine, 0.1 μ M aminopterin, and 17.5 μ M thymidine (HAT). Seeding densities ranged from 100 to 100,000 cells/ml (20 to 20,000 cells/well), depending on the test chemicals evaluated. Concurrently, cells were plated in 200 μ l per well into 96-microwell flat bottom plates at a density of 8 cells/ml (1.6 cells/well) without HAT to assess the cloning efficiency (CE). After 21 days of incubation, the number of colonies in both the CE and HAT plates was recorded. CE was calculated using Eq. 1 based on the Poisson distribution⁵¹, where EW represents the number of wells without colonies, TW represents the total number of wells, and N is the average number of cells per well ($N = 1.6$) in the CE plates.

$$CE = -\ln(EW / TW) / N \quad (1)$$

Relative survival (%) was determined by comparing the CE values of chemical-treated cells to those of the solvent control. The TK revertant frequency was calculated using Eq. 2 also based on the Poisson distribution. Here, N corresponds to the number of cells per well ($N = 20$ to 20,000) in the HAT plates. The results were statistically analyzed using Dunnett's test and compared with solvent control values.

$$TK \text{ revertant frequency} = [-\ln(EW / TW) / N] / \text{treated CE} \quad (2)$$

Bisulfite sequencing

To assess the basal DNA methylation status at the *TK* promoter region of TK6 and mTK6 cell lines, 1×10^6 cells were collected and washed with phosphate-buffered saline (PBS). To evaluate DNA methylation patterns following treatment with DNMT inhibitors, 10 ml of mTK6 cells at a concentration of 250,000 cells/ml were treated with 0.1 μ M 5-azadC or 2 μ M GSK-3484862 at 37°C for 24 h. The cells were seeded into 96-well flat-bottom plates containing HAT, as described in the “epi-TK assay” section. The revertant colonies were then cultivated to collect 1×10^6 cells, which were washed with PBS. Spontaneous revertant colonies were also cultivated from HAT plates seeded with mTK6 cells without chemical treatment. Genomic DNA was extracted from the collected cells (1×10^6) using the Nucleospin Tissue kit (Macherey-Nagel). The extracted DNA, dissolved in 50 μ L H₂O (2 μ g), was treated with 5.5 μ L of 2 M NaOH and incubated at 37°C for 15 min. Subsequently, 30 μ L of 10 mM hydroquinone and 520 μ L of 2 M sodium metabisulfite were added to the mixture, followed by incubation at 50°C for 16 h. The bisulfite-converted DNA was purified using the Wizard DNA Clean-Up System (Promega)

and subjected to PCR amplification using EpiTaq HS (TAKARA). A 451 bp DNA fragment containing the TK promoter region was amplified using primers listed in Supplementary Table S2. The resulting PCR products were ligated into the pTA2 Vector using the Target Clone TA cloning system (Toyobo Co., Ltd.). The ligation mixture was transformed into *Escherichia coli* TOP10 cells, and recombinant clones were verified by Sanger sequencing.

Chromatin immunoprecipitation-quantitative PCR (ChIP-qPCR)

To assess H3K27Ac and H3K4me3 levels following TPA exposure, cells were treated with 20 ng/ml TPA at 37 °C for 24 h. After treatment, the cells were washed twice with RMPI-1640 medium and cultured exponentially for 3 days to allow phenotypic expression. A total of 3×10^6 cells were then cross-linked with 1% formaldehyde at room temperature for 10 min. The cross-linking reaction was terminated by adding 125 mM glycine. Following this, cells were washed with PBS and resuspended in 300 µl sonication buffer (10 mM Tris-HCl (pH8.0), 2 mM EDTA, 0.25% SDS). DNA was fragmented by sonication, and the resulting chromatin was incubated at 4 °C for 16 h with specific antibodies (anti-H3K27Ac monoclonal antibody (AB_2793797, ACTIVE MOTIF) and anti-H3K4me3 monoclonal antibody (ab8580, abcam)) and Protein A Sepharose 4 beads (Cytiva). The Sepharose beads were washed, and the immunoprecipitated DNA was eluted using elution buffer (10 mM Tris-HCl (pH 8.0), 1 mM EDTA, 1% SDS, 0.3 µg/ml Proteinase K) at 65 °C for 6 h. Purification of DNA was performed using the NucleoSpin Gel and PCR Clean-up kit (Macherey-Nagel). The abundance of immunoprecipitated DNA was quantified using the Thunderbird® Next SYBR qPCR Mix (Toyobo Co., Ltd.) with specific primers listed in Supplementary Table S2.

Western blotting

Total cell extracts were fractionated on gradient 5–20% SDS-polyacrylamide gels and transferred onto PVDF membranes. The membranes were blocked with 3% skim milk before incubation with primary antibodies. To detect H3K27Ac, Histone H3, and GAPDH, membranes were incubated overnight at 4 °C in Hikari A solution (Nacalai Tesque) with the following antibodies: 1:1000 dilution of anti-H3K27Ac monoclonal antibody (AB_2793797, ACTIVE MOTIF), 1:1000 dilution of anti-Histone H3 monoclonal antibody (gifted from Dr. Kimura), or 1:1000 dilution of anti-GAPDH monoclonal antibody (sc-32233, Santa Cruz). After washing with tris-buffered saline containing 0.05% Tween 20, the membranes were incubated with a 1:4000 dilution of anti-mouse IgG or anti-rat IgG conjugated to horseradish peroxidase (Cytiva) in Hikari B solution (Nacalai Tesque). The chemiluminescent signal were detected using Chemi-Lumi One Super (Nacalai Tesque).

Data availability

The transcriptome data raw files have been deposited to the DDBJ with accession number PRJDB19707: <https://www.ncbi.nlm.nih.gov/bioproject/?term=PRJDB19707>.

Received: 11 December 2024; Accepted: 25 February 2025

Published online: 05 March 2025

References

1. Organisation for Economic Co-operation and Development. Environment Directorate, Organisation for Economic Co-operation and Development, Joint Meeting of the Chemicals Committee and the Working Party on Chemicals Pesticides and Biotechnology & Inter-Organization Programme for the Sound Management of Chemicals. *Guidance for conducting retrospective studies on socio-economic analysis*. (OECD, 1999).
2. Sharma, S., Kelly, T. K. & Jones, P. A. Epigenetics in cancer. *Carcinogenesis* **31**, 27–36. <https://doi.org/10.1093/carcin/bgp220> (2010).
3. Baccarelli, A. & Bollati, V. Epigenetics and environmental chemicals. *Curr. Opin. Pediatr.* **21**, 243–251. <https://doi.org/10.1097/mo.0b013e32832925cc> (2009).
4. Eglén, R. M. & Reisine, T. Screening for compounds that modulate epigenetic regulation of the transcriptome: an overview. *J. Biomol. Screen.* **16**, 1137–1152. <https://doi.org/10.1177/1087057111417871> (2011).
5. Miyamoto, K. & Ushijima, T. [DNA methylation and cancer—DNA methylation as a target of cancer chemotherapy]. *Gan Kagaku Ryoho.* **30**, 2021–2029 (2003).
6. Bolden, J. E., Peart, M. J. & Johnstone, R. W. Anticancer activities of histone deacetylase inhibitors. *Nat. Rev. Drug Discov.* **5**, 769–784. <https://doi.org/10.1038/nrd2133> (2006).
7. Hou, L., Zhang, X., Wang, D. & Baccarelli, A. Environmental chemical exposures and human epigenetics. *Int. J. Epidemiol.* **41**, 79–105. <https://doi.org/10.1093/ije/dyr154> (2012).
8. Hernandez, L. G., van Steeg, H., Luijten, M. & van Benthem, J. Mechanisms of non-genotoxic carcinogens and importance of a weight of evidence approach. *Mutat. Res.* **682**, 94–109. <https://doi.org/10.1016/j.mrrev.2009.07.002> (2009).
9. Johnson, R. L. et al. A quantitative high-throughput screen identifies potential epigenetic modulators of gene expression. *Anal. Biochem.* **375**, 237–248. <https://doi.org/10.1016/j.ab.2007.12.028> (2008).
10. Cui, Y. et al. A Recombinant reporter system for monitoring reactivation of an endogenously DNA hypermethylated gene. *Cancer Res.* **74**, 3834–3843. <https://doi.org/10.1158/0008-5472.CAN-13-2287> (2014).
11. Chen, Y. et al. c-Myc activates BRCA1 gene expression through distal promoter elements in breast cancer cells. *BMC Cancer.* **11**, 246. <https://doi.org/10.1186/1471-2407-11-246> (2011).
12. Okochi-Takada, E. et al. Establishment of a high-throughput detection system for DNA demethylating agents. *Epigenetics* **13**, 147–155. <https://doi.org/10.1080/15592294.2016.1267887> (2018).
13. Sugiyama, K., Takamune, M., Furusawa, H. & Honma, M. Human DNA methyltransferase gene-transformed yeasts display an inducible flocculation inhibited by 5-aza-2'-deoxycytidine. *Biochem. Biophys. Res. Commun.* **456**, 689–694. <https://doi.org/10.1016/j.bbrc.2014.12.032> (2015).
14. Sugiyama, K. I., Furusawa, H., Shimizu, M., Gruz, P. & Honma, M. Epigenetic mutagen as histone modulator can be detected by yeast flocculation. *Mutagenesis* **31**, 687–693. <https://doi.org/10.1093/mutage/gew041> (2016).
15. Sugiyama, K. I., Kinoshita, M., Furusawa, H., Sato, K. & Honma, M. Epigenetic effect of the Mycotoxin Fumonisin B1 on DNA methylation. *Mutagenesis* **36**, 295–301. <https://doi.org/10.1093/mutage/geab019> (2021).
16. Yasui, M. et al. Weight of evidence approach using a TK gene mutation assay with human TK6 cells for follow-up of positive results in Ames tests: a collaborative study by MMS/JEMS. *Genes Environ.* **43**, 7. <https://doi.org/10.1186/s41021-021-00179-1> (2021).

17. Schisler, M. R., Gollapudi, B. B. & Moore, M. M. Evaluation of U. S. National toxicology program (NTP) mouse lymphoma assay data using international workshop on genotoxicity tests (IWGT) and the organization for economic Co-Operation and development (OECD) criteria. *Environ. Mol. Mutagen.* **59**, 829–841. <https://doi.org/10.1002/em.22250> (2018).
18. Ibrahim, M. A. et al. Enhancing the sensitivity of the thymidine kinase assay by using DNA repair-deficient human TK6 cells. *Environ. Mol. Mutagen.* **61**, 602–610. <https://doi.org/10.1002/em.22371> (2020).
19. Sassa, A. et al. Follow-up genotoxicity assessment of Ames-positive/equivocal chemicals using the improved thymidine kinase gene mutation assay in DNA repair-deficient human TK6 cells. *Mutagenesis* **36**, 331–338. <https://doi.org/10.1093/mutage/geab025> (2021).
20. Sassa, A. et al. Comparative study of cytotoxic effects induced by environmental genotoxins using XPC- and CSB-deficient human lymphoblastoid TK6 cells. *Genes Environ.* **41**, 15. <https://doi.org/10.1186/s41021-019-0130-y> (2019).
21. Pflueger, C. et al. A modular dCas9-SunTag DNMT3A epigenome editing system overcomes pervasive off-target activity of direct fusion dCas9-DNMT3A constructs. *Genome Res.* **28**, 1193–1206. <https://doi.org/10.1101/gr.233049.117> (2018).
22. Liu, Q. & Gong, Z. The coupling of epigenome replication with DNA replication. *Curr. Opin. Plant. Biol.* **14**, 187–194. <https://doi.org/10.1016/j.pbi.2010.12.001> (2011).
23. Ohmori, K., Kamei, A., Watanabe, Y. & Abe, K. Gene expression over time during cell transformation due to Non-Genotoxic carcinogen treatment of bhas 42 cells. *Int. J. Mol. Sci.* **23**. <https://doi.org/10.3390/ijms23063216> (2022).
24. Kuan, P. F., Huebert, D., Gasch, A. & Keles, S. A non-homogeneous hidden-state model on first order differences for automatic detection of nucleosome positions. *Stat. Appl. Genet. Mol. Biol.* **8**. <https://doi.org/10.2202/1544-6115.1454> (2009).
25. Boyle, A. P. et al. High-resolution mapping and characterization of open chromatin across the genome. *Cell* **132**, 311–322. <https://doi.org/10.1016/j.cell.2007.12.014> (2008).
26. Giresi, P. G., Kim, J., McDaniell, R. M., Iyer, V. R. & Lieb, J. D. FAIRE (Formaldehyde-Assisted isolation of regulatory Elements) isolates active regulatory elements from human chromatin. *Genome Res.* **17**, 877–885. <https://doi.org/10.1101/gr.5533506> (2007).
27. Buenrostro, J. D., Giresi, P. G., Zaba, L. C., Chang, H. Y. & Greenleaf, W. J. Transposition of native chromatin for fast and sensitive epigenomic profiling of open chromatin, DNA-binding proteins and nucleosome position. *Nat. Methods.* **10**, 1213–1218. <https://doi.org/10.1038/nmeth.2688> (2013).
28. Lieberman-Aiden, E. et al. Comprehensive mapping of long-range interactions reveals folding principles of the human genome. *Science* **326**, 289–293. <https://doi.org/10.1126/science.1181369> (2009).
29. Zhu, X. et al. Thymidine kinase 1 Silencing retards proliferative activity of pancreatic cancer cell via E2F1-TK1-P21 axis. *Cell. Prolif.* **51**, e12428. <https://doi.org/10.1111/cpr.12428> (2018).
30. Karlseder, J., Rotheneder, H. & Wintersberger, E. Interaction of Sp1 with the growth- and cell cycle-regulated transcription factor E2F. *Mol. Cell. Biol.* **16**, 1659–1667. <https://doi.org/10.1128/MCB.16.4.1659> (1996).
31. Policarpi, C., Munafo, M., Tsagkris, S., Carlini, V. & Hackett, J. A. Systematic epigenome editing captures the context-dependent instructive function of chromatin modifications. *Nat. Genet.* **56**, 1168–1180. <https://doi.org/10.1038/s41588-024-01706-w> (2024).
32. Han, M. H., Issagulova, D. & Park, M. Interplay between epigenome and 3D chromatin structure. *BMB Rep.* **56**, 633–644. <https://doi.org/10.5483/BMBRep.2023-0197> (2023).
33. Azevedo Portilho, N. et al. The DNMT1 inhibitor GSK-3484862 mediates global demethylation in murine embryonic stem cells. *Epigenetics Chromatin.* **14**, 56. <https://doi.org/10.1186/s13072-021-00429-0> (2021).
34. Kiianitsa, K., Zhang, Y. & Maizels, N. Treatment of human cells with 5-aza-dC induces formation of PARP1-DNA covalent adducts at genomic regions targeted by DNMT1. *DNA Repair. (Amst)*. **96**, 102977. <https://doi.org/10.1016/j.dnarep.2020.102977> (2020).
35. Bouche, M. et al. TPA-induced differentiation of human rhabdomyosarcoma cells: expression of the myogenic regulatory factors. *Exp. Cell. Res.* **208**, 209–217. <https://doi.org/10.1006/excr.1993.1239> (1993).
36. Radaszkiewicz, K. A. et al. 12-O-Tetradecanoylphorbol-13-acetate increases cardiomyogenesis through PKC/ERK signaling. *Sci. Rep.* **10**, 15922. <https://doi.org/10.1038/s41598-020-73074-4> (2020).
37. Kolb, T. M. & Davis, M. A. The tumor promoter 12-O-tetradecanoylphorbol 13-acetate (TPA) provokes a prolonged morphologic response and ERK activation in Tsc2-null renal tumor cells. *Toxicol. Sci.* **81**, 233–242. <https://doi.org/10.1093/toxsci/kfh183> (2004).
38. Dunn, K. L. et al. Increased genomic instability and altered chromosomal protein phosphorylation timing in HRAS-transformed mouse fibroblasts. *Genes Chromosomes Cancer.* **48**, 397–409. <https://doi.org/10.1002/gcc.20649> (2009).
39. Khan, D. H. et al. Mitogen-induced distinct epialleles are phosphorylated at either H3S10 or H3S28, depending on H3K27 acetylation. *Mol. Biol. Cell.* **28**, 817–824. <https://doi.org/10.1091/mbc.E16-08-0618> (2017).
40. Kamiya, T., Goto, A., Kurokawa, E., Hara, H. & Adachi, T. Cross talk mechanism among EMT, ROS, and histone acetylation in phorbol Ester-Treated human breast Cancer MCF-7 cells. *Oxid. Med. Cell. Longev.* **2016**, 1284372. <https://doi.org/10.1155/2016/1284372> (2016).
41. Huang, W., Mishra, V., Batra, S., Dillon, I. & Mehta, K. D. Phorbol ester promotes histone H3-Ser10 phosphorylation at the LDL receptor promoter in a protein kinase C-dependent manner. *J. Lipid Res.* **45**, 1519–1527. <https://doi.org/10.1194/jlr.M400088-JLR200> (2004).
42. Cataisson, C., Pearson, A. J., Torgerson, S., Nedospasov, S. A. & Yuspa, S. H. Protein kinase C alpha-mediated chemotaxis of neutrophils requires NF-kappa B activity but is independent of TNF alpha signaling in mouse skin in vivo. *J. Immunol.* **174**, 1686–1692. <https://doi.org/10.4049/jimmunol.174.3.1686> (2005).
43. Medeiros, R., Otuki, M. F., Avellar, M. C. & Calixto, J. B. Mechanisms underlying the inhibitory actions of the pentacyclic triterpene alpha-amyrin in the mouse skin inflammation induced by phorbol ester 12-O-tetradecanoylphorbol-13-acetate. *Eur. J. Pharmacol.* **559**, 227–235. <https://doi.org/10.1016/j.ejphar.2006.12.005> (2007).
44. Vezzani, B. et al. Epigenetic regulation: A link between inflammation and carcinogenesis. *Cancers.* **14**. <https://doi.org/10.3390/cancers14051221> (2022).
45. Shanmugam, M. K. & Sethi, G. Role of epigenetics in inflammation-associated diseases. *Subcell. Biochem.* **61**, 627–657. https://doi.org/10.1007/978-94-007-4525-4_27 (2013).
46. Bode, K. A. et al. Histone deacetylase inhibitors decrease Toll-like receptor-mediated activation of Proinflammatory gene expression by impairing transcription factor recruitment. *Immunology* **122**, 596–606. <https://doi.org/10.1111/j.1365-2567.2007.02678.x> (2007).
47. Reddy, P. et al. Histone deacetylase Inhibition modulates indoleamine 2,3-dioxygenase-dependent DC functions and regulates experimental graft-versus-host disease in mice. *J. Clin. Invest.* **118**, 2562–2573. <https://doi.org/10.1172/JCI34712> (2008).
48. Ali, M. N. et al. The HDAC inhibitor, SAHA, prevents colonic inflammation by suppressing Pro-inflammatory cytokines and chemokines in DSS-induced colitis. *Acta Histochem. Cytochem.* **51**, 33–40. <https://doi.org/10.1267/ahc.17033> (2018).
49. Bhattacharya, A. et al. MUC1-C intersects chronic inflammation with epigenetic reprogramming by regulating the set1a compass complex in cancer progression. *Commun. Biol.* **6**, 1030. <https://doi.org/10.1038/s42003-023-05395-9> (2023).
50. Mali, P. et al. RNA-guided human genome engineering via Cas9. *Science* **339**, 823–826. <https://doi.org/10.1126/science.1232033> (2013).
51. Furth, E. E., Thilly, W. G., Penman, B. W., Liber, H. L. & Rand, W. M. Quantitative assay for mutation in diploid human lymphoblasts using microtiter plates. *Anal. Biochem.* **110**, 1–8. [https://doi.org/10.1016/0003-2697\(81\)90103-2](https://doi.org/10.1016/0003-2697(81)90103-2) (1981).

Acknowledgements

We are grateful to Dr. Hiroshi Honda (Kao Corporation) and Dr. Takayuki Fukuda (Bozo Research Center)

for their helpful comments and discussions. We also thank Dr. Hiroshi Kimura (Tokyo Institute of Technology, Japan) for generously providing the antibody used to identify histone H3.

Author contributions

H.Y., M.O., M.Y., and A.S. conceptualized the research, H.Y., M.O., K.Y., M.Y., M.H., K.S., K.U., and A.S. participated in study discussions and experimental design. H.Y., M.O., K.Y., A.C., A.U., M.Y., and A.S. carried out the experiments and analyzed the data. A.S. authored the manuscript and all authors reviewed and approved the final manuscript.

Declarations

Competing interests

The authors declare no competing interests.

Additional information

Supplementary Information The online version contains supplementary material available at <https://doi.org/10.1038/s41598-025-92121-6>.

Correspondence and requests for materials should be addressed to M.Y. or A.S.

Reprints and permissions information is available at www.nature.com/reprints.

Publisher's note Springer Nature remains neutral with regard to jurisdictional claims in published maps and institutional affiliations.

Open Access This article is licensed under a Creative Commons Attribution-NonCommercial-NoDerivatives 4.0 International License, which permits any non-commercial use, sharing, distribution and reproduction in any medium or format, as long as you give appropriate credit to the original author(s) and the source, provide a link to the Creative Commons licence, and indicate if you modified the licensed material. You do not have permission under this licence to share adapted material derived from this article or parts of it. The images or other third party material in this article are included in the article's Creative Commons licence, unless indicated otherwise in a credit line to the material. If material is not included in the article's Creative Commons licence and your intended use is not permitted by statutory regulation or exceeds the permitted use, you will need to obtain permission directly from the copyright holder. To view a copy of this licence, visit <http://creativecommons.org/licenses/by-nc-nd/4.0/>.

© The Author(s) 2025